

Abstract

A variety of nonthermal characteristics like kinetic, e.g., temperature, anisotropies and suprathermal populations are revealed by the in-situ observations in the solar wind indicating quasistationary states of plasma particles out of thermal equilibrium. Large deviations from isotropy generate kinetic instabilities and growing fluctuating fields which should be more efficient than collisions in limiting the anisotropy and explain the anisotropy limits reported by the observations. The present work proposes to decode the principal instabilities driven by the temperature anisotropy of electrons and protons in the solar wind, and contrast the instability thresholds with the bounds observed at 1 AU for the temperature anisotropy. The analysis focuses on the electromagnetic instabilities driven by the anisotropic protons and invokes for the first time a dynamical model to capture the interplay with the anisotropic electrons by correlating the effects of these two species of plasma particles, dominant in the solar wind.

Motivation

The instabilities of electromagnetic oscillatory modes driven by the proton anisotropy i.e., electromagnetic ion-cyclotron instability (EMICI) and proton firehose instability (PFHI) are mainly studied using simplified models assuming protons bi-Maxwellian distributed and minimizing the effects of electrons considering them isotropic [1] and references therein) or considering them anisotropic with constant values independent of the proton properties [2, 3, 4]. In these studies the instability thresholds do not provide a good agreement with the limits of proton temperature anisotropy observed in the solar wind, being markedly lower than these limits, which instead appear to be better described by the thresholds of the mirror and aperiodic PFH instabilities [5, 6]. Here we present the results of a refined dynamical analysis of the periodic instabilities, which take into account the correlations between the anisotropies of electrons and protons as indicated by the observations.

Governing Dispersion Relations

For a collisionless and homogeneous electron-proton plasma, the dispersion relations for the electromagnetic modes propagating in a direction parallel to the stationary magnetic field read [1]

$$\frac{c^2 k^2}{\omega^2} = 1 + \sum_{\alpha=e,p} \frac{\omega_{p,\alpha}^2}{\omega^2} \left[\frac{\omega}{k u_{\alpha,\parallel}} Z_{\alpha,\eta}(\xi_{\alpha,\eta}^{\pm}) + (A_{\alpha} - 1) \left\{ 1 + \xi_{\alpha,\eta}^{\pm} Z_{\alpha,\eta}(\xi_{\alpha,\eta}^{\pm}) \right\} \right], \quad (1)$$

where ω is the wave-frequency, k is the wave-number, c is the speed of light, $\omega_{p,\alpha}^2 = 4\pi n_{\alpha} e^2 / m_{\alpha}$ are the plasma frequencies for protons (subscript $\alpha = p$) and electrons (subscript $\alpha = e$), $A_{\alpha} = T_{\alpha,\perp} / T_{\alpha,\parallel}$ are the temperature anisotropies, \pm denote the circular polarizations, right-handed (RH) and left-handed (LH), respectively. $Z_{\alpha,\eta}(\xi_{\alpha,\eta}^{\pm})$ may denote either the plasma dispersion function for (bi)-Maxwellian distributed plasmas (subscript $\eta = M$), or the modified dispersion function for Kappa distributed plasmas (subscript $\eta = \kappa$), and $u_{\alpha,\parallel}$ are the corresponding thermal velocities. The dispersion relation simplifies, in terms of the normalized quantities,

$$\tilde{k}^2 = A_p - 1 + \frac{A_p (\tilde{\omega} \pm 1) \mp 1}{\tilde{k} \sqrt{\beta_{p,\parallel}}} Z_{p,\eta} \left(\frac{\tilde{\omega} \pm 1}{\tilde{k} \sqrt{\beta_{p,\parallel}}} \right) + \mu (A_e - 1) + \mu \frac{A_e (\tilde{\omega} \mp \mu) \pm \mu}{\tilde{k} \sqrt{\mu \beta_{e,\parallel}}} Z_{e,\eta} \left(\frac{\tilde{\omega} \mp \mu}{\tilde{k} \sqrt{\mu \beta_{e,\parallel}}} \right) \quad (2)$$

where $\tilde{\omega} = \omega / \Omega_p$, $\tilde{k} = kc / \omega_{p,p}$, $\mu = m_p / m_e$ is the proton/electron mass ratio, $\beta_{\alpha,\parallel} = 8\pi n_{\alpha} k_B T_{\alpha,\parallel} / B^2$ are the parallel plasma betas for protons (subscript $\alpha = p$) or electrons (subscript $\alpha = e$).

Now we assume $A_e = A_p^{\delta}$, with a correlation index δ , eventually indicated by the observations.

The unstable solutions

The interplay of the electrons and protons anisotropies can change the linear dispersive and instability properties as follows

• Effect of the electron anisotropy $A_e = A_p^{\delta}$ on PFHI

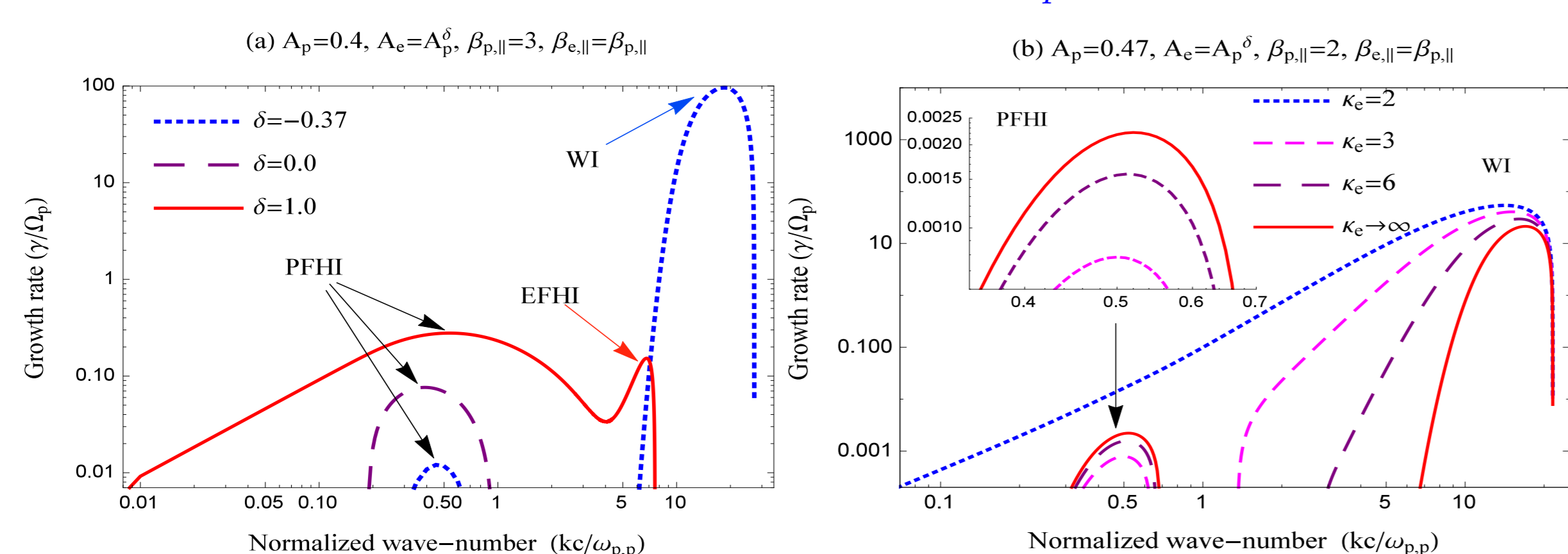


Figure 1: Effects of electron anisotropy (panel a) and the power-index κ_c (panel b) on the PFHI growth rate

• Effect of the electron anisotropy $A_e = A_p^{\delta}$ on EMICI

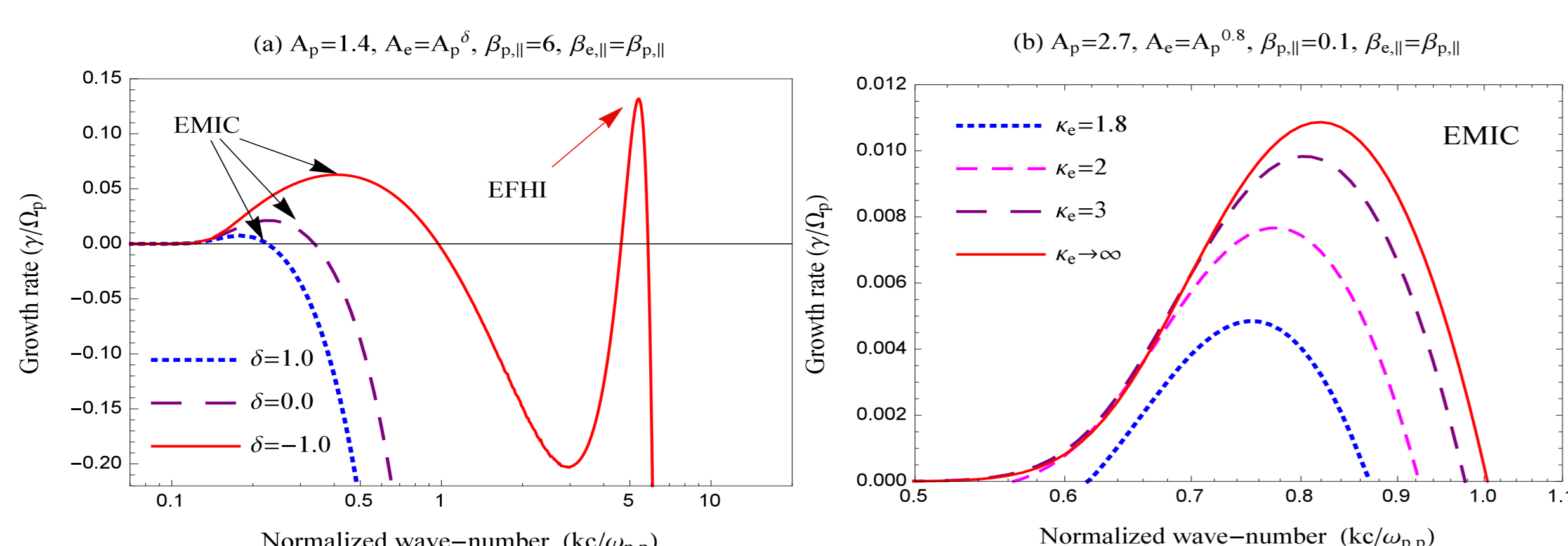


Figure 2: Effects of electron anisotropy (panel a) and the power-index κ_c (panel b) on EMIC growth rate

The instability thresholds

In order to have a more comprehensive view on the interplay of the anisotropic electrons and protons in destabilizing the unstable modes, we have derived the anisotropy thresholds for the maximum growth rates $\gamma_m / \Omega_p = 10^{-3}$. These thresholds are obtained with an inverse correlation law between the temperature anisotropy A_p and parallel plasma beta $\beta_{p,\parallel}$ as

$$A_p = 1 + \frac{a}{(\beta_{p,\parallel} - \beta_0)^b} \quad (3)$$

where a , b , and β_0 are the fitting parameters.

• Effect of the electron anisotropy $A_e = A_p^{\delta}$ on the PFHI

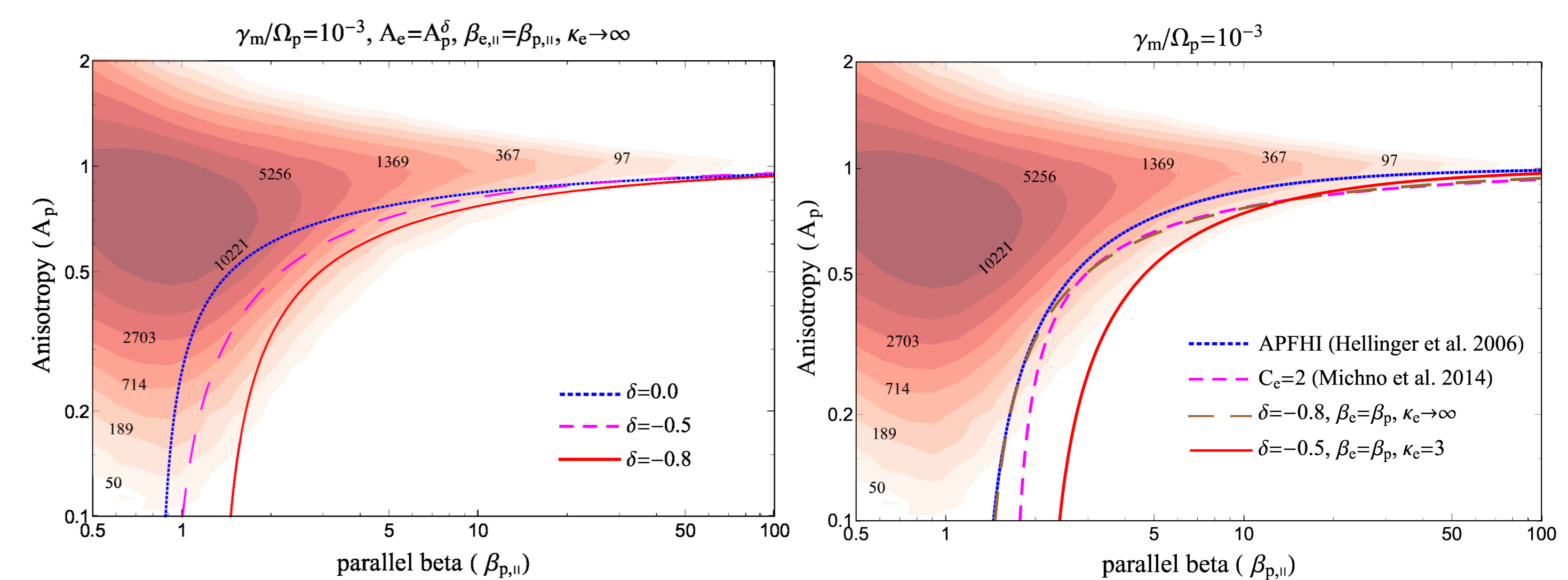


Figure 3: Effect of the electron anisotropy $A_e = A_p^{\delta}$ on PFHI threshold (panel a), and a comparison with previously published results (panel b)

• Effect of the electron anisotropy $A_e = A_p^{\delta}$ on the EMICI

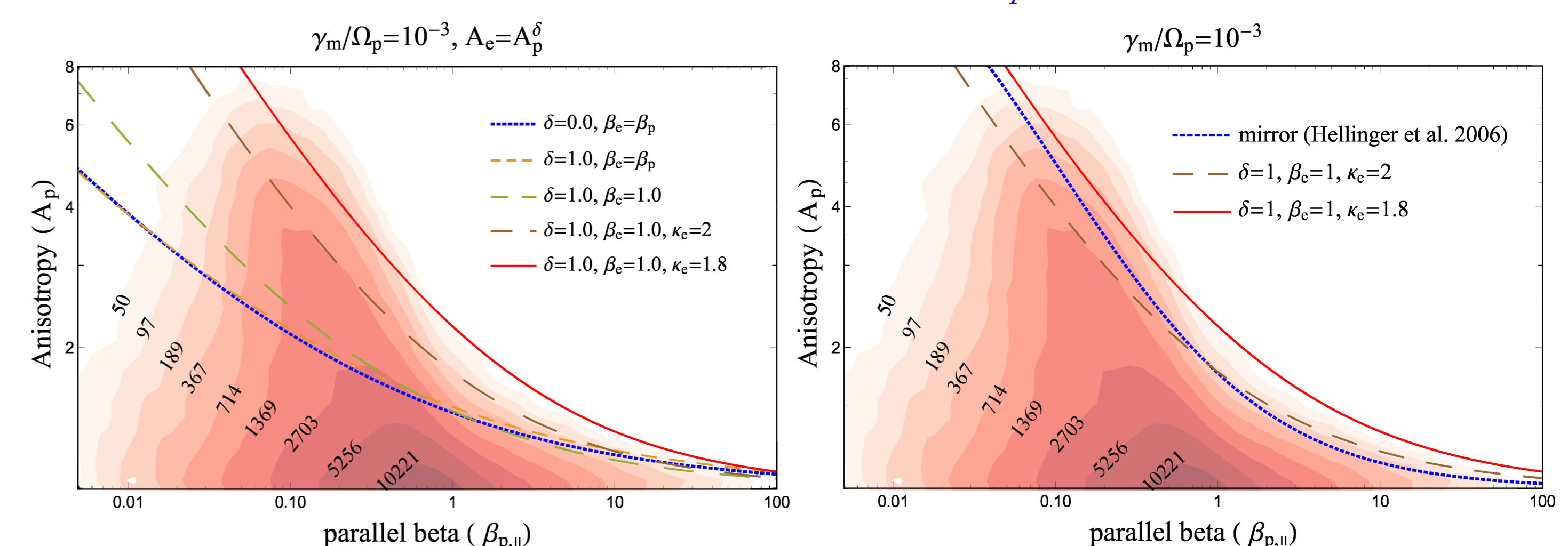


Figure 4: Effect of the electron anisotropy $A_e = A_p^{\delta}$ on EMIC threshold (panel a), and a comparison with previously published results (panel b)

Conclusions

We have proposed a refined dynamical model for the cumulative effects of the anisotropic electrons and protons to describe the effects of the resulting instabilities in the solar wind. The growth rates display two distinct peaks (Figure 1,2), one peak triggered by the anisotropic protons (A_p) at lower wave-numbers, and a second peak directly stimulated by the electron anisotropy (A_e), and the power-index κ_c . For the PFHI, the anisotropy thresholds are increased, e.g., to higher plasma beta $\beta_{p,\parallel}$ with decreasing the δ -index and the power-index κ_c . For the EMICI, the instability thresholds are again increased, e.g., to higher anisotropies A_p by increasing the δ -index and the electron suprathermal populations. Compared to the previous results obtained by Michno et al.[2], and Hellinger et. al.[6] the instability thresholds from a more realistic approach (red solid line in Figures 3,4) show a better alignment with the limits of the proton anisotropy in the solar wind.

References

- [1] Gary, S.P., 1993, *Theory of space plasma microinstabilities*, Cambridge Univ. Press.
- [2] Michno, M. J., Lazar, M., Yoon, P. H., & Schlickeiser, R. 2014, *ApJ*, 781, 49
- [3] Shaaban, S. M., et al., 2015, *ApJ*, 814, 34.
- [4] Shaaban, S. M., et al., 2016, *A&SS*, 361, 1-12.
- [5] Bale, S. D., Kasper, J. C., Howes, G. G., Quataert, E., Salem, C., & Sundkvist, D. 2009, *PhRvL*, 103, 211101
- [6] Hellinger, P., Trávníček, P., Kasper, J. C., & Lazarus, A. J. 2006, *GeoRL*, 33